Belt, Tiina; Venäläinen, Martti; Altgen, Michael; Harju, Anni; Rautkari, Lauri

Extractive concentrations and cellular-level distributions change radially from outer to inner heartwood in Scots pine

Published in:
Tree Physiology

DOI:
10.1093/treephys/tpaa166

Published: 01/06/2021

Document Version
Peer-reviewed accepted author manuscript, also known as Final accepted manuscript or Post-print

Extractive concentrations and cellular level distributions change radially from outer to inner heartwood in Scots pine

Radial changes in heartwood extractives

Tiina Belt[a,b*], Martti Venäläinen[c], Michael Altgen[b,d], Anni Harju[c], Lauri Rautkari[b]

[a] Natural Resources Institute Finland, Production Systems, Tietotie 2, 02150 Espoo, Finland

[b] Aalto University School of Chemical Engineering, Department of Bioproducts and Biosystems, P.O.Box 16300, 00076 Aalto, Finland

[c] Natural Resources Institute Finland, Production Systems, Vipusenkuja 5, 57200 Savonlinna, Finland

[d] Department of Biology, Institute of Wood Science, Wood Physics, Universität Hamburg, Leuschnerstraße 91 c, 21031 Hamburg, Germany

*corresponding author

tiina.belt@luke.fi

Abstract

The heartwood of many wood species is rich in extractives, which improve the wood material's resistance to biological attack. Their concentration is generally higher in outer than inner heartwood, but the exact radial changes in aging heartwood remain poorly characterised. This investigation studied these radial changes in detail in Scots pine (*Pinus sylvestris* L.), using radial sample sequences prepared from three different trees. Stilbene and resin acid contents were first measured from bulk samples, after which the extractive contents of individual heartwood annual rings were investigated using Raman spectroscopy and fluorescence microscopy. Raman imaging and fluorescence microscopy were also used to study the cellular level distributions of extractives in different annual rings. Although there were substantial differences between the trees, the content and distribution of stilbenes seemed to follow a general radial trend. The results suggest that stilbenes are absorbed into heartwood tracheid cell walls from small stilbene-rich extractive deposits over several years and then eventually transform into non-extractable compounds in aging heartwood. Resin acids followed no consistent radial trends, but their content was strongly connected to the frequency of large extractive deposits in latewood tracheid lumens. The results highlight the variability of heartwood extractives: their content and distribution vary not only between trees but also between and even within the annual rings of a single tree. This high variability is likely to have important effects on the properties of heartwood and the utilisation of heartwood timber.

Keywords: durability, extractives, pinosylvin, phenolic, terpenoid

Introduction

Heartwood is dead tissue found in the inner layers of the tree trunk, formed from aging sapwood in a process where the innermost sapwood parenchyma cells die. Heartwood formation is characterised by the accumulation of heartwood extractives (Taylor et al. 2002), which are a large and diverse group of mostly small molecular weight compounds. Heartwood extractives often possess antifungal and other bioactive properties, and in many tree species, their presence increases the heartwood's resistance to degradation by wood decaying fungi (Hillis 1987, Taylor et al. 2002).

The conversion of sapwood to heartwood takes place in a narrow zone between the two, called the transition zone. The heartwood extractives are either synthesised directly in the transition zone by parenchyma cells, or their precursors are synthesised in the aging sapwood by the parenchyma cells and then converted to heartwood extractives in the transition zone (reviewed by Kampe and Magel 2013, Celedon and Bohlmann 2018). Recent evidence suggests that a small portion of cells may also survive the heartwood formation process and continue synthesising extractives in the heartwood (Celedon and Bohlmann 2018). After synthesis and parenchyma cell death, the extractives are released into the surrounding wood tissues. Microscopic investigations have revealed the progressive spread of heartwood extractives from ray parenchyma cells into surrounding tracheids (Kuroda et al. 2014) and the movement of extractives from ray parenchyma to tracheids/fibres through pit connections (Nagasaki et al. 2002, Zhang et al. 2004). Once deposited into the heartwood, the extractives can be found in the cell walls and middle lamellae of heartwood tracheids and as small deposits or large occlusions in the lumens of tracheids, ray parenchyma and axial parenchyma (Nagasaki et al. 2002, Zhang et al. 2004, Matsushita et al. 2012, Kuroda et al. 2014, Belt et al. 2017, Felhofer et al. 2018).

63 The concentration of heartwood extractives generally increases rapidly at the heartwood-
64 sapwood border and then decreases from outer to inner heartwood (Bergström et al. 1999,
65 DeBell et al. 1999, Nagasaki et al. 2002, Gierlinger and Wimmer 2004, Ekeberg et al. 2006).
66 The decrease has been attributed both to increasing extractive formation with tree age (DeBell
67 et al. 1999, Gierlinger and Wimmer 2004) and to secondary reactions (oxidation,
68 polymerisation, binding to lignin) in aging heartwood that decrease the concentration of the
69 original extractives over time (Helm et al. 1997, Bergström et al. 1999, Shimizu et al. 2017).
70 However, most of the information on radial changes in extractive content have been obtained
71 using bulk measurements, which means that the data is low in spatial resolution. Furthermore,
72 no information is available on the radial changes in the cellular level distributions of
73 extractives.

74 The current investigation set out to study the radial changes in heartwood extractives in detail,
75 using Scots pine (*Pinus sylvestris* L.) as the example wood species. Chromatographic bulk
76 chemical analysis, Raman spectroscopy, confocal Raman spectroscopy imaging, and
77 fluorescence microscopy were used to monitor extractives in radial sample sequences prepared
78 from three different trees. The objectives of the investigation were to determine how the (i)
79 concentrations and (ii) cellular level distributions of extractives change from the heartwood-
80 sapwood border to the innermost heartwood annual rings and to (iii) obtain clues about the
81 processes governing these changes. These variations are important to understand because both
82 extractive content and distribution affect many important heartwood properties, including
83 decay resistance (Hillis 1987, Taylor et al. 2002).

84

Materials and methods

Sample preparation

Scots pine (*Pinus sylvestri*s L.) wood samples were prepared from three bottom logs obtained from three different trees grown in eastern (logs A and B) or southern Finland (log C). Log A had 122 annual rings (65 heartwood rings), log B 74 annual rings (32 heartwood rings) and log C 74 annual rings (25 heartwood rings). The logs were stored frozen protected from light and desiccation until use. To prepare radial sample sequences for chemical analysis and imaging, a disc approx. 50 mm in thickness (longitudinal) was cut from each log, after which a 15 mm wide (tangential) strip was cut from bark to bark through the pith. After visually identifying the heartwood-sapwood border based on the moisture difference, 15 mm wide (radial) heartwood blocks were cut from the strips starting from the first annual ring designated as heartwood (heartwood ring 1) and continuing towards the pith. The pith itself was excluded from sampling. A total of nine heartwood samples covering heartwood rings 1-56 were prepared from log A, three covering heartwood rings 1-27 from log B and three covering heartwood rings 1-21 from log C. One 15 mm wide block was also cut from each strip from the sapwood side of the border. Finally, all the prepared blocks were cut across the grain to produce one 15 mm thick imaging sample and one 30 mm thick chemical analysis sample. Sample preparation and the prepared samples are shown in Figure 1.

[Figure 1]

Extraction and extractive analysis

The chemical analysis samples were cut into thin sticks with a razor blade, freeze dried and ground to a powder in a Wiley mill (mesh 20). Portions (0.15 g) of each powder were then solvent extracted with MeOH (2 x 5 ml) for 30 min at 45°C in a sonicator. Three replicate

extractions were performed per sample. The extraction solvent contained 0.1 mg/ml of diethyl stilbestrol as internal standard. After extraction, 25 µl aliquots of each extract were placed into a vial and the solvent evaporated under vacuum. The dry extracts were then dissolved in 75 µl of pyridine and trimethylsilylated at 70°C for 20 min after the addition of 25 µl of N,O-Bis(trimethylsilyl)trifluoroacetamide with 10% chlorotrimethylsilane. The composition of the extracts was analysed by GC-FID (Shimadzu GC 2010 Plus) and GC-MS (Shimadzu GCMS-QP2010 SE). Both analyses used a HP-5 column (30 m x 0.23 mm i.d., 0.25 µm film thickness), helium as the carrier gas (1 ml/min), and the following oven temperature program: 2 min at 100°C, 10°C/min to 200°C, 5°C/min to 280°C, and 5 min at 280°C. Mass spectra (50-700 m/z) were recorded at 70 eV. The extractive compounds were first identified by GC-MS and then quantitatively analysed by GC-FID using the known concentration of internal standard for quantitation.

Raman spectroscopy and imaging

Cross sections approx. 25 µm in thickness were cut from the imaging samples using a rotary microtome. The cross-sections were placed on microscope slides with a drop of deionized water, covered with glass coverslips (0.17 mm thickness) and edge-sealed with nail polish. Raman images and spectra were acquired using a WITec alpha 300 RA Raman microscope equipped with a 532 nm frequency doubled Nd:YAG laser (used at 30 mW) and a DU970-BV EMCCD camera behind a 600 lines/mm grating.

Raman images were acquired from all heartwood samples, from the earlywood and latewood regions of selected annual rings. The images were acquired using a 100x oil objective (NA 1.25, coverslip correction 0.17 mm) and a 0.3s integration time. The image size was 25x25 μm^2 with 100 lines per image and 100 points per line. False-colour images describing the

distribution of heartwood stilbenes were generated by calculating the integrated intensity of the stilbene C=C stretch band at 1628-1645 rel. cm^{-1} (see Figure S1 available as Supplementary Data at *Tree Physiology* online). Background was subtracted from the integrated intensity by setting the spectral intensity to zero at four wavelengths above and below the wavenumber range of interest.

Single spectra were also collected from all samples, from four separate locations on both the latewood and earlywood regions of every other annual ring in heartwood rings 1-30 and from every fifth annual ring after ring 30. Sapwood spectra were obtained from the two closest annual rings to the heartwood-sapwood border. The spectra were obtained from the secondary cell wall region using a 20x air objective (NA 0.4), a 0.3s integration time and ten accumulations per spectrum. The integrated intensity of the stilbene band was calculated for every spectrum. Due to variations in the overall intensity of the individual spectra, the intensities were normalised by dividing with the integrated intensity of the aromatic ring stretch band at 1580-1620 rel. cm^{-1}. All data processing and integrations were performed using WITec suite 4 software.

Fluorescence microscopy

Cross sections approx. 25 µm in thickness were again cut from the imaging samples using a rotary microtome and placed on microscope slides. Most of the cross sections were directly embedded in water and sealed with nail polish as above, but some were first extracted with acetone (5 x 200 µl) on the slides and then embedded in water. The native and extracted cross sections were observed with an Olympus BX53 microscope using a 20x air objective (NA 0.5) and UV excitation (330-385 nm excitation filter, 420 nm long pass emission filter). Fluorescence images sized 352 x 264 μm^2 were collected from all samples, from the earlywood

and latewood regions of every other annual ring in heartwood rings 1-30 and from every fifth annual ring after ring 30. Sapwood images were obtained from the two closest annual rings to the heartwood-sapwood border. Two to four images were collected from both earlywood and latewood in each ring using a QImaging Micropublisher RTV 3.3 camera. Image acquisition was controlled by ImagePro software. Constant image settings were used for all samples. The fluorescence intensity of each image was calculated by first calculating the total intensity of all pixels where the intensity exceeded a threshold value and then dividing that with the number of pixels where the threshold was exceeded to exclude empty cell lumens.

Results

Extractive content of bulk samples

Scots pine heartwood extractives consist of stilbenes, resin acids, free fatty acids and small amounts of other compounds, while the sapwood extractives consist primarily of triglycerides and smaller amounts of other compounds such as resin acids (Willför et al. 2003). To investigate the radial changes in extractives, the bulk concentrations of extractives were first determined chromatographically in the radial sample sequences obtained from the three logs. Since stilbenes and resin acids are the most abundant extractives found in heartwood and the ones connected to decay resistance (Harju et al. 2002, Venäläinen et al. 2004, Leinonen et al. 2008), the analysis focused on these compounds. Their total concentrations are given in Figure 2, while the concentrations of the individual compounds can be found in Table S2 (available as Supplementary Data at *Tree Physiology* online). Other compounds found in the heartwood extracts are summarised in Figure S3 (available as Supplementary Data at *Tree Physiology* online).

[Figure 2]

The total concentration of stilbenes ranged between 0.6 and 19.2 mg/g in the heartwood samples, with similar maximum concentrations (13.9-19.2 mg/g) recorded in all three logs. The radial sampling sequence revealed that the stilbene content of log A increased from the first heartwood sample to the second and then decreased from the third sample onwards. The heartwood stilbene content also decreased from the second to the third sample in log B but increased in log C, which contained fewer annual rings in the first two samples than logs A and B. No stilbenes were detected in the sapwood samples.

The concentration of resin acids showed more log to log variation than that of the stilbenes and revealed no consistent radial trends. In log A the resin acid concentration peaked in the first heartwood sample and remained low (3.8-7.6 mg/g) in the subsequent samples, whereas in log B the concentration was low in the first heartwood sample (4.2 mg/g) and increased towards the third and final sample (25.1 mg/g). Log C had a higher resin acid content than the other logs, with a maximum concentration of 60.8 mg/g in the second heartwood sample. The resin acid content of all sapwood samples was low (1.2-3.3 mg/g).

In addition to stilbenes and resin acids, the heartwood samples also contained fatty acids and other compounds detectable by GC (see Figure S3 available as Supplementary Data at *Tree Physiology* online). The fatty acid content of log A (maximum content 13.1 mg/g) was higher than that of logs B and C (maximum content <5 mg/g). The non-fatty acid compounds detected in log A appeared in the older heartwood samples and increased in concentration towards the pith. These compounds were identified as monosaccharides, primarily arabinose and galactose, likely derived from heartwood arabinogalactan (Fischer and Höll 1992, Willför and Holmbom 2004). Small amounts of other unidentified compounds were detected in the log B and C samples.

Extractives in different annual rings

Cellular level distributions

To further investigate the radial changes in heartwood extractives, Raman and fluorescence images were collected from different annual rings and analysed to explore the changes in extractive content and cellular level distribution. Raman imaging was used to visualise stilbenes, which produce a unique band at 1628-1645 rel. cm^{-1} in the Raman spectrum of heartwood (Holmgren et al. 1999, Belt et al. 2017, Felhofer et al. 2018, see also Figure S1 available as Supplementary Data at *Tree Physiology* online). The stilbene band is absent in sapwood (Belt et al. 2017, Felhofer et al. 2018, see also Figure S1). False-colour Raman images from selected heartwood annual rings produced by integrating the stilbene band are given in Figure 3. Fluorescence microscopy was used to visualise all UV-fluorescent heartwood compounds, which include stilbenes and resin acids. Stilbenes produce blue fluorescence under UV-excitation, although the excitation wavelengths used in this experiment (330-385 nm) are higher than their excitation maximum at approx. 320 nm (Harju et al. 2009, Antikainen et al. 2012). Resin acid mixtures have been shown to produce blue/green fluorescence under UV-excitation (Donaldson et al. 2019), but the fluorescence properties of the individual acids remain poorly understood. Fluorescence images from selected annual rings are shown in Figure 4.

[Figure 3]

[Figure 4]

Raman imaging indicated the presence of stilbenes in heartwood tracheid cell walls, middle lamellae and lumens in all three logs. Both small deposits and large lumen-filling deposits were present in the latewood tracheid lumens, while only small deposits were found in the earlywood tracheid lumens. The Raman spectra of the small and large deposits showed that the small

deposits consisted mostly of stilbenes, while the large deposits also contained resin acids and/or fatty acids (see Figure S4 available as Supplementary Data at *Tree Physiology* online). Fluorescence imaging also showed the presence of deposits in heartwood tracheid lumens as well as in the lumens of ray cells. The tracheid and ray cell deposits (as well as resin canals, see Figure S5 available as Supplementary Data at *Tree Physiology* online) were brightly fluorescent, while the tracheid cell walls and middle lamellae showed weaker fluorescence. The fluorescence signal from the cell walls and middle lamellae is likely to include contributions from lignin, which is also autofluorescent under UV excitation (Donaldson et al. 2010). In agreement with Raman imaging, the fluorescence images showed both small and large deposits in latewood tracheid lumens and only small deposits in earlywood tracheids. The colour of fluorescence in both the tracheid and ray cell deposits ranged from dark purple-blue to blue to bright blue-green (see Figure S5 available as Supplementary Data at *Tree Physiology* online), indicating variation in their composition.

Changes in Raman and fluorescence intensity

The Raman and fluorescence images collected from different radial positions on the three logs generally shared the same features, but there was substantial variation in the Raman/fluorescence intensity and the frequency at which the features appeared in each image. To investigate the changes in intensity and thus extractive content across the annual rings, Raman and fluorescence intensity data were extracted. Data for comprehensive Raman intensity analysis was obtained by collecting individual Raman spectra from earlywood and latewood secondary cell walls on every other (heartwood rings 1-30) or every fifth (rings 30+) annual ring. Raman spectra were also obtained from sapwood. The intensity of the stilbene band at 1628-1645 rel. cm^{-1} was integrated, and due to variations in the overall intensity of the spectra, the stilbene band intensities were normalised by dividing with the integrated intensity

253 of the aromatic ring stretch band (1580-1620 cm^{-1}), which contains contributions from both
254 lignin and stilbenes (Felhofer et al. 2018). Fluorescence intensity data was extracted from the
255 heartwood and sapwood fluorescence images by calculating the total intensity of all pixels
256 where the intensity exceeded a threshold value and then dividing that with the number of pixels
257 where the threshold was exceeded. This procedure was used to exclude empty cell lumens and
258 to minimise the effects of differences in cell number and size. The Raman and fluorescence
259 intensity data are presented in Figure 5.

260 [Figure 5]

261 The local stilbene concentrations revealed by the Raman intensity data were correlated
262 (R^2=0.768) with the chromatographic bulk measurement results (see Figure S6 available as
263 Supplementary Data at *Tree Physiology* online). The differences between the Raman intensity
264 and bulk results were at least partly due to differences between the methods: the bulk
265 measurements measure the stilbene content of the entire sample block, whereas the Raman
266 method measures the intensity from isolated secondary cell wall locations on the sample
267 surface. The Raman intensity data provided more detailed information on the radial variations
268 in stilbene content than the bulk measurements and revealed notable differences between the
269 three logs. In log A the intensity increased progressively in the first heartwood rings, reached
270 its maximum around the tenth ring and then began to decrease, whereas in log B the intensity
271 remained low in the first heartwood rings, rapidly increased around the tenth ring and then
272 fluctuated around this value. In log C the intensity continued to increase until approx. the 20^{th}
273 heartwood ring. The stilbene band was absent in all sapwood spectra.

274 The radial trends revealed by the fluorescence intensity data were different from those shown
275 by the Raman intensity measurements. The difference between the Raman and fluorescence
276 results was particularly noticeable in the case of log A, where the fluorescence results indicated

277 that the extractive-derived intensity continued to increase until the 50th heartwood annual ring
278 instead of decreasing after the tenth ring. In log B the fluorescence intensity results showed a
279 moderate increase in intensity from the 13th annual ring to the 21st instead of the rapid increase
280 around the tenth annual ring as indicated by the Raman intensity data. Log C was the only log
281 where the radial patterns derived from Raman and fluorescence data were similar. The
282 fluorescence intensity results did not correlate with the chromatographically determined
283 stilbene content nor with resin acid content (see Figure S6 available as Supplementary Data at
284 *Tree Physiology* online), suggesting the presence of other fluorescent compounds in Scots pine
285 heartwood.

286 To investigate the nature of the increasing fluorescence, new sections were produced from the
287 heartwood samples and solvent extracted on the microscope slides. Fluorescence images were
288 then collected from approximately every tenth annual ring on the extracted sections and
289 fluorescence intensity data extracted as before. The post-extraction fluorescence intensities are
290 shown in Figure 6, while Figure S7 (available as Supplementary Data at *Tree Physiology*
291 online) provides a direct comparison between the fluorescence intensities of sapwood and
292 native and extracted heartwood. Although the applied extraction procedure appeared to
293 efficiently remove all extractives deposits from ray and tracheid lumens, the fluorescence
294 intensity of the extracted heartwood samples was never reduced to the level of sapwood. In all
295 three logs, the intensity of non-extractable heartwood fluorescence increased towards the pith.
296 In the innermost annual rings the increased non-extractable fluorescence may be due to juvenile
297 wood: juvenile wood shares characteristics with compression wood, which has been shown to
298 have a higher fluorescence intensity than normal wood due to differences in lignin structure
299 (Donaldson et al. 2010). However, since juvenile wood is limited to the 20 or so innermost
300 annual rings in Scots pine (Sauter et al. 1999), its presence cannot account for the increasing
301 non-extractable intensity of rings 20 and 30 in log A.

[Figure 6]

Changes in deposits

In addition to variations in Raman and fluorescence intensity, the images collected from different annual rings on the three logs (Figures 3 and 4) showed variations in the distribution of extractives, particularly in the occurrence of different types of extractive deposits. Thus, to investigate the radial changes in the distribution of extractives, we analysed the deposits seen on the fluorescence images collected from different annual rings. The small and large deposits found in tracheid lumens were analysed by calculating their frequency (what percentage of cells in each image contained a deposit), while the deposits found in rays were analysed by estimating the degree of ray filling on a scale of 1-5 (1 = 0-20% filling, 2 = 20-40% filling, 3 = 40-60% filling, 4 = 60-80% filling, and 5 = 80-100% filling). Ray filling was estimated by measuring the length of each ray and the approximate total length of the fluorescent material within the ray. The deposit frequencies and ray fill ratings at different annual ring intervals are given in Figure 7. Annual ring intervals rather than individual rings were used in deposit analysis to highlight the overall trends rather than variations between individual rings.

[Figure 7]

The small deposits found in earlywood and latewood tracheid lumens showed a relatively consistent radial trend in all three logs. Their abundance increased from the first annual ring interval (heartwood rings 1-9) to the second (rings 10-19) and then began to decline. Earlywood had a higher frequency of small deposits than latewood and showed a more prominent radial trend. In contrast to the small deposits, the large latewood deposits and the ray filling degree showed no consistent radial trends. The frequency of large deposits was highest in log C, followed by rings 10-19 and 20-29 in log B and rings 1-9 in log A, while the ray filling degree

declined towards the pith in log A, increased in log B and remained constant in log C. Both the small and the large deposits showed substantial local variation in all logs, with some annual rings containing areas of both high and low deposit abundance (see Figure S8 available as Supplementary Data at *Tree Physiology* online). The ray filling degree showed substantial local variation as well, and in many fluorescence images, completely full rays could be seen adjacent to completely empty rays.

Discussion

The chromatographic bulk measurements (Figure 2) revealed that the stilbene content of heartwood increased from the first sample at the heartwood-sapwood border to the second in all three logs. The stilbene content of log A then decreased from the third sample onwards, reaching very low concentrations in the innermost samples. The radially decreasing stilbene content of log A is in agreement with previous reports (Venäläinen et al. 2003), which have shown that the stilbene content of old Scots pine logs is lower in inner than outer heartwood. The low stilbene content of the innermost heartwood samples in the older log A but not in the younger logs B and C suggests that the lower stilbene content of inner heartwood may be due to secondary reactions in aging heartwood rather than to increasing production with increasing tree age, although more data is needed to confirm this hypothesis.

The concentration of resin acids in turn showed high variation between and within the logs and revealed no consistent radial trends. The high variation and the lack of consistent trends suggest that the resin acid content of Scots pine heartwood is controlled by a different mechanism than its stilbene content. Transcriptomic analyses have shown that stilbenes are synthesised directly in the transition zone, while resin acids are synthesised primarily in the sapwood and then

transported into heartwood (Lim et al. 2016). The processes controlling the synthesis and transport of resin acids are unknown, but the data collected here suggest that their activity can vary substantially during a tree's life. Although the concentration of resin acids showed no consistent radial trends, potential secondary reactions cannot be ruled out since their effects might be masked by the other variations.

Raman images collected from different annual rings on the three logs (Figure 3) revealed the presence of stilbenes in heartwood tracheid lumens, cell walls and middle lamellae, in agreement with previous reports (Belt et al. 2017, Felhofer et al. 2018, Belt et al. 2019). Although all the images collected from different radial positions showed the same general cellular level distributions, there were substantial variations in the overall Raman intensity and extractive deposit frequency. The radial variations in cell wall stilbene content were investigated in detail by extracting stilbene band intensity data from single Raman spectra collected from different annual rings (Figure 5a-c). Although there were substantial differences between the three logs, the Raman intensity data clearly showed that the cell wall concentration of stilbenes increased for some 10-20 annual rings after their first appearance. The increasing concentration is likely to be due to continued deposition of stilbenes into the cell walls, although continued synthesis due to residual enzyme activity cannot be excluded. Small amounts of active phenol-oxidising enzymes have been previously extracted from the heartwood of pines (Shain and Mackay 1973, Fagerstedt et al. 1998). Cell wall stilbene content declined substantially in the inner heartwood rings in log A but not in logs B and C, presumably due to the relatively young age of their inner heartwood.

Fluorescence images collected from different annual rings (Figure 4) also showed the presence of extractives in tracheid lumens, cell walls and middle lamellae, as well as in the lumens of ray cells. Analogous to the Raman intensity analysis, fluorescence intensity data was extracted from the images to obtain information on the radial variations in all UV-fluorescent compounds

374 (Figure 5d-f). However, the radial patterns revealed by the fluorescence intensity data were
375 different from the Raman intensity data, particularly in the case of log A. Further fluorescence
376 intensity data obtained from images collected from solvent extracted sections (Figure 6)
377 showed that the inner heartwood rings contained increasing amounts of non-extractable
378 fluorescent material. In combination with the decreasing stilbene content of log A (Figures 2
379 and 5) and the lack of potential stilbene conversion products in the log A extracts (Figure S3),
380 the data suggest that the stilbenes are converted to non-extractable products in aging
381 heartwood. Non-extractable non-lignin polymers (Dellus et al. 1997a,b) and lignin-bound
382 extractives (Helm et al. 1997) have been previously detected in the heartwood of other wood
383 species.

384 The variations in the frequency of extractive deposits were investigated by counting the small
385 and large tracheid deposits found on the fluorescence images and by estimating the degree of
386 ray filling (Figure 7). The abundance of the small stilbene-rich deposits (see Figure S4) varied
387 between and within annual rings, but there was a relatively consistent radial trend: their
388 frequency increased from the first investigated annual ring interval to the second and then
389 began to decline. Their decreasing frequency suggests that stilbenes spread in the heartwood
390 in the form of droplets, which are then absorbed into the wood material over time. The
391 absorption of extractives into the cell walls from droplets agrees with the Raman intensity data
392 (Figure 5), which showed that the cell wall stilbene content increased for 10-20 annual rings
393 depending on the log. Thus, the small deposit data shows that it was not only the concentration
394 of stilbenes but also their distribution that continuously changed in the heartwood from the
395 outermost to the innermost annual rings.

396 In contrast to the small deposits, the large deposits found in latewood showed no consistent
397 radial trends. Their frequency suggests that their numbers are connected to local resin acid
398 content (see Figure 2b) rather than to radial position in the log. The large deposits contain both

399 stilbenes and resin acids (see Figure S4), which means that the local concentration of resin
400 acids also influences the cellular level distribution of stilbenes. The ray deposits also showed
401 no consistent radial trends, and like the large deposits, their trends suggest that ray filling is
402 connected to local resin acid content. However, since the ray fill ratings were not higher in log
403 C than the other logs, it appears that the ray filling degree is not simply a function of resin acid
404 content.

405 The radial trends in stilbene content and distribution are summarised in Figure 8. Although
406 there were differences between the three trees, the results of this investigation suggest that
407 stilbenes undergo changes in the radial direction from the heartwood-sapwood border to inner
408 heartwood. However, it should be noted that extractive distributions, and most likely also
409 concentrations, vary not only from one annual ring to another but also within annual rings (see
410 Figure S8). The samples used in this investigation were only 15 mm wide, and it is reasonable
411 to assume that even greater variation would be seen within annual rings if the entire tree cross-
412 section was examined. The high variation in extractive content and distribution in the radial
413 direction and within annual rings is likely to have important effects on extractive-dependent
414 heartwood properties such as resistance to biological attack. Even if the overall extractive
415 content of a piece of heartwood is high, the sample may be susceptible because the areas of
416 high extractive content are unable to afford protection to the areas of low extractive content.

417 [Figure 8]

418

419 Conclusions

420 The analyses performed on three Scots pine trees revealed some interesting trends in the
421 content and cellular level distribution of Scots pine heartwood extractives. The data indicated

that the stilbene content of heartwood increases for several annual rings from the heartwood-sapwood border and then begins to decrease, along with a decrease in the abundance of stilbene-rich deposits and an increase in non-extractable fluorescence. Resin acids showed no consistent trends, but their content was found to be strongly linked to the frequency of large deposits in latewood tracheid lumens. The results of this experiment reveal the high variability of Scots pine heartwood extractives: extractive content and distribution vary not only from one tree to another but also from one annual ring to another in the radial direction and even within individual annual rings. This high variability has important effects on the properties and utilisation of heartwood, because it means that any given piece of heartwood is likely to show substantial variation in its properties. The effect is particularly significant in terms of biological resistance because the areas of low extractive abundance are likely to act as points of weakness in the heartwood defences.

Supplementary Data

Supplementary Data.docx

Conflict of Interest

None declared

Funding

T.B acknowledges financial support by the Jenny and Antti Wihuri foundation.

Acknowledgements

This work made use of Aalto University Bioeconomy Facilities.

Authors' Contributions

T.B. designed the study, M.V. acquired the wood materials and M.A. prepared the samples, T.B. performed the experimental work, T.B. analysed the data and wrote the manuscript with contributions from all co-authors, L.R. supervised the work.

References

Antikainen J, Hirvonen T, Kinnunen J, Hauta-Kasari M (2012) Heartwood detection for Scotch pine by fluorescence image analysis. Holzforschung 66:877-881

Belt T, Altgen M, Mäkelä M, Hänninen T, Rautkari L (2019) Cellular level chemical changes in Scots pine heartwood during incipient brown rot decay. Sci Rep 9:5188

Belt T, Keplinger T, Hänninen T, Rautkari L (2017) Cellular level distributions of Scots pine heartwood and knot heartwood extractives revealed by Raman spectroscopy imaging. Ind Crop Prod 108:327-335

Bergström B, Gustafsson G, Gref R, Ericsson A (1999) Seasonal changes of pinosylvin distribution in the sapwood/heartwood boundary of *Pinus sylvestris*. Trees-Struct Funct 14:65-71

Celedon JM, Bohlmann J (2018) An extended model of heartwood secondary metabolism informed by functional genomics. Tree Physiol 38:311-319

DeBell J, Morrel J, Gartner B (1999) Within-stem variation in tropolone content and decay resistance of second-growth western redcedar. For Sci 45:101-107

462 Dellus V, Mila I, Scalbert A, Menard C, Michon V, duPenhoat C (1997) Douglas-fir
463 polyphenols and heartwood formation. Phytochemistry 45:1573-1578

464 Dellus V, Scalbert A, Janin G (1997) Polyphenols and colour of Douglas fir heartwood.
465 Holzforschung 51:291-295

466 Donaldson LA, Singh A, Raymond L, Hill S, Schmitt U (2019) Extractive distribution in
467 *Pseudotsuga menziesii*: effects on cell wall porosity in sapwood and heartwood. IAWA
468 Journal 40:721-740

469 Donaldson L,A., Radotić K, Kalauzi A, Djikanović D, Jeremić M (2010) Quantification of
470 compression wood severity in tracheids of *Pinus radiata* D. Don using confocal fluorescence
471 imaging and spectral deconvolution. J Struct Biol 169:106-115

472 Ekeberg D, Flæte PO, Eikenes M, Fongen M, Naess-Andresen C (2006) Qualitative and
473 quantitative determination of extractives in heartwood of Scots pine (*Pinus sylvestris* L.) by
474 gas chromatography. J Chromatogr A 1109:267-272

475 Fagerstedt K, Saranpää P, Piispanen R (1998) Peroxidase activity, isoenzymes and
476 histological localisation in sapwood and heartwood of Scots pine (*Pinus sylvestris* L.). J For
477 Res 3:43-47

478 Felhofer M, Prats-Mateu B, Bock P, Gierlinger N (2018) Antifungal stilbene impregnation:
479 transport and distribution on the micron-level. Tree Physiol 38:1526-1537

480 Fischer C, Höll W (1992) Food reserves of scots pine (*Pinus sylvestris* L.) II. Seasonal
481 changes and radial distribution of carbohydrate and fat reserves in pine wood. Trees 6:147–
482 155

483 Gierlinger N, Wimmer R (2004) Radial distribution of heartwood extractives and lignin in
484 mature European larch. Wood Fiber Sci 36:387-394

485 Harju AM, Kainulainen P, Venäläinen M, Tiitta M, Viitanen H (2002) Differences in resin
486 acid concentration between brown-rot resistant and susceptible Scots pine heartwood.
487 Holzforschung 56:479-486

488 Harju AM, Venäläinen M, Laakso T, Saranpää P (2009) Wounding response in xylem of
489 Scots pine seedlings shows wide genetic variation and connection with the constitutive
490 defence of heartwood. Tree Physiol 29:19-25

491 Helm RF, Ranatunga TD, Chandra M (1997) Lignin-hydrolyzable tannin interactions in
492 wood. J Agric Food Chem 45:3100-3106

493 Hillis WE (1987) Heartwood and tree exudates. Springer-Verlag, Berlin

494 Holmgren A, Bergström B, Gref R, Ericsson A (1999) Detection of pinosylvins in solid wood
495 of Scots pine using Fourier transform Raman and infrared spectroscopy. J Wood Chem
496 Technol 19:139-150

497 Kampe A, Magel E (2013) New insights into heartwood and heartwood formation. In:
498 Fromm J (ed) Cellular aspects of wood formation. Springer, Berlin, pp 71-95

499 Kuroda K, Fujiwara T, Hashida K, Imai T, Kushi M, Saito K, Fukushima K (2014) The
500 accumulation pattern of ferruginol in the heartwood-forming *Cryptomeria japonica* xylem as
501 determined by time-of-flight secondary ion mass spectrometry and quantity analysis. Ann Bot
502 113:1029-1036

503 Leinonen A, Harju AM, Venäläinen M, Saranpää P, Laakso T (2008) FT-NIR spectroscopy
504 in predicting the decay resistance related characteristics of solid Scots pine (*Pinus sylvestris*
505 L.) heartwood. Holzforschung 62:284-288

506 Lim KJ, Paasela T, Harju A, Venäläinen M, Paulin L, Auvinen P, Kärkkäinen K, Teeri TH
507 (2016) Developmental changes in Scots pine transcriptome during heartwood formation.
508 Plant Physiol 172:1403-1417

509 Matsushita Y, Jang I, Imai T, Takama R, Saito K, Masumi T, Lee S, Fukushima K (2012)
510 Distribution of extracts including 4,8-dihydroxy-5-methoxy-2-naphthaldehyde in *Diospyros*
511 *kaki* analyzed by gas chromatography-mass spectrometry and time-of-flight secondary ion
512 mass spectrometry. Holzforschung 66:705-709

513 Nagasaki T, Yasuda S, Imai T (2002) Immunohistochemical localization of agatharesinol, a
514 heartwood norlignan, in *Cryptomeria japonica*. Phytochemistry 60:461-466

515 Sauter U,H, Mutz R, Munro BD (1999) Determining juvenile-mature wood transition in scots
516 pine using latewood density. Wood Fiber Sci 31:416-425

517 Shain L, Mackay GJF (1973) Phenol-oxidizing enzymes in the heartwood of *Pinus radiata*.
518 Forest Sci 12:153-155

519 Shimizu Y, Iki T, Imai T (2017) Radial distribution of monomeric, dimeric and trimeric
520 norlignans and their polymerization in *Cryptomeria japonica* heartwood. Holzforschung
521 71:705-712

522 Taylor AM, Gartner BL, Morrell JJ (2002) Heartwood formation and natural durability - A
523 review. Wood Fiber Sci 34:587-611

524 Venäläinen M, Harju AM, Saranpää P, Kainulainen P, Tiitta M, Velling P (2004) The
525 concentration of phenolics in brown-rot decay resistant and susceptible Scots pine heartwood.
526 Wood Sci Technol 38:109-118

527 Venäläinen M, Harju AM, Kainulainen P, Viitanen H, Nikulainen H (2003) Variation in the
528 decay resistance and its relationship with other wood characteristics in old Scots pines. Ann
529 For Sci 60:409-417

530 Willför S, Hemming J, Reunanen M, Holmbom B (2003) Phenolic and lipophilic extractives
531 in Scots pine knots and stemwood. Holzforschung 57:359-372

532 Willför S, Holmbom B (2004) Isolation and characterisation of water soluble polysaccharides
533 from Norway spruce and Scots pine. Wood Sci Technol 38:173–179

534 Zhang CH, Fujita M, Takabe K (2004) Extracellular diffusion pathway for heartwood
535 substances in *Albizia julibrissin* Durazz. Holzforschung 58:495-500

List of figures

Figure 6. Fluorescence intensity (ex: 330-385 nm, em: 420- nm) after extraction in the earlywood and latewood regions of approximately every tenth heartwood annual ring in logs A, B and C. Ring 1 is the first ring at the sapwood-heartwood border designated as heartwood. The fluorescence intensity of sapwood has been subtracted from the heartwood fluorescence values

Figure 7. Frequency of small and large earlywood (EW) and latewood (LW) deposits in fluorescence images collected from different annual ring intervals in logs A, B and C (a), and the degree of ray filling in fluorescence images collected from different annual ring intervals in logs A, B and C given as ray fill rating, where 1 = 0-20% filling, 2 = 20-40% filling, 3 = 40-60% filling, 4 = 60-80% filling, and 5 = 80-100% filling (b)

Figure 8. Stilbenes in Scots pine heartwood. Stilbene content increases for some 10-20 annual rings from the heartwood-sapwood border and then begins to decrease, along with a decrease in the abundance of stilbene-rich small deposits in tracheid lumens and an increase in non-extractable cell wall fluorescence. The large deposits found in latewood tracheid lumens contain mixtures of stilbenes and resin acids, and their abundance increases when the local resin acid content increases

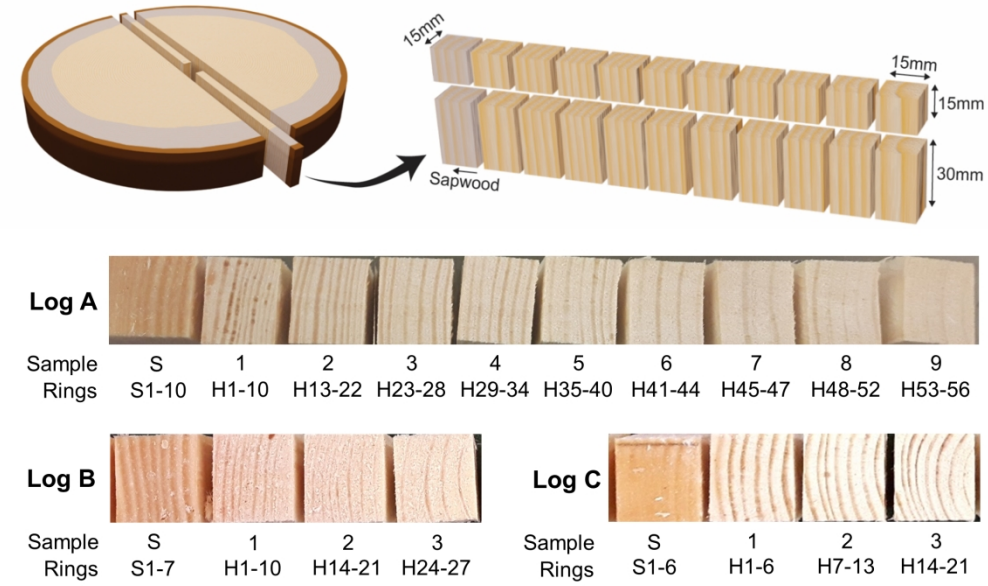

Figure 1. Sample preparation and the final sapwood and heartwood samples prepared from logs A, B and C

199x119mm (300 x 300 DPI)

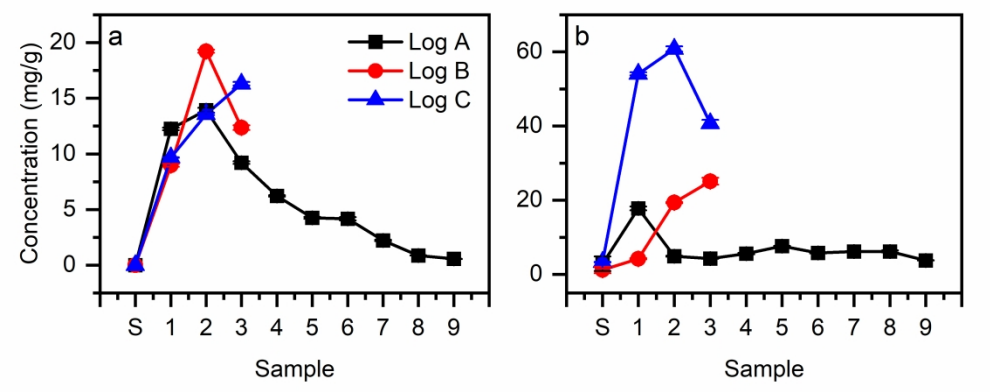

Figure 2. Concentrations (mg/g wood) of stilbenes (a) and resin acids (b) in the sapwood (S) and heartwood (1-9) samples from logs A, B and C

179x70mm (600 x 600 DPI)

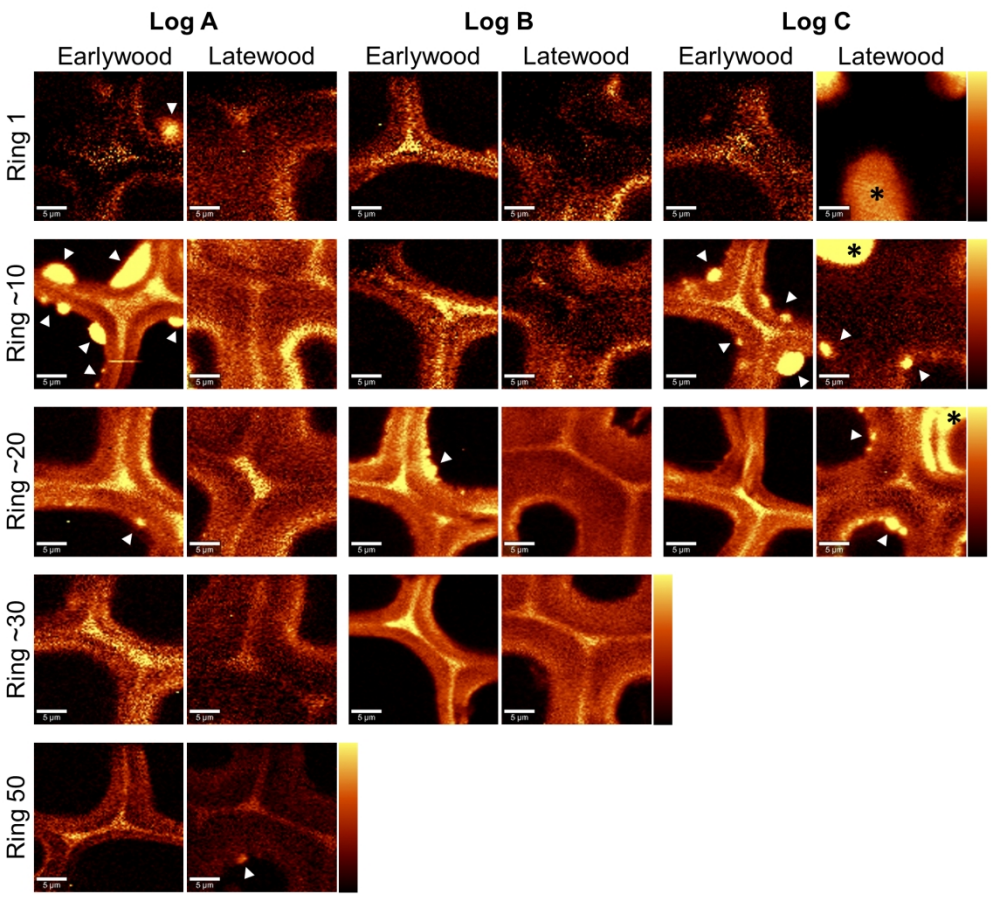

Figure 3. Raman images showing the distribution of stilbenes (integration of the stilbene C=C stretch band at 1628-1645 rel. cm^{-1}) in the earlywood and latewood regions of different heartwood annual rings in logs A, B and C. Ring 1 is the first ring at the sapwood-heartwood border designated as heartwood. Arrowheads indicate the locations of small deposits and asterisks the locations of large deposits. Scale bar is 5 µm

171x155mm (300 x 300 DPI)

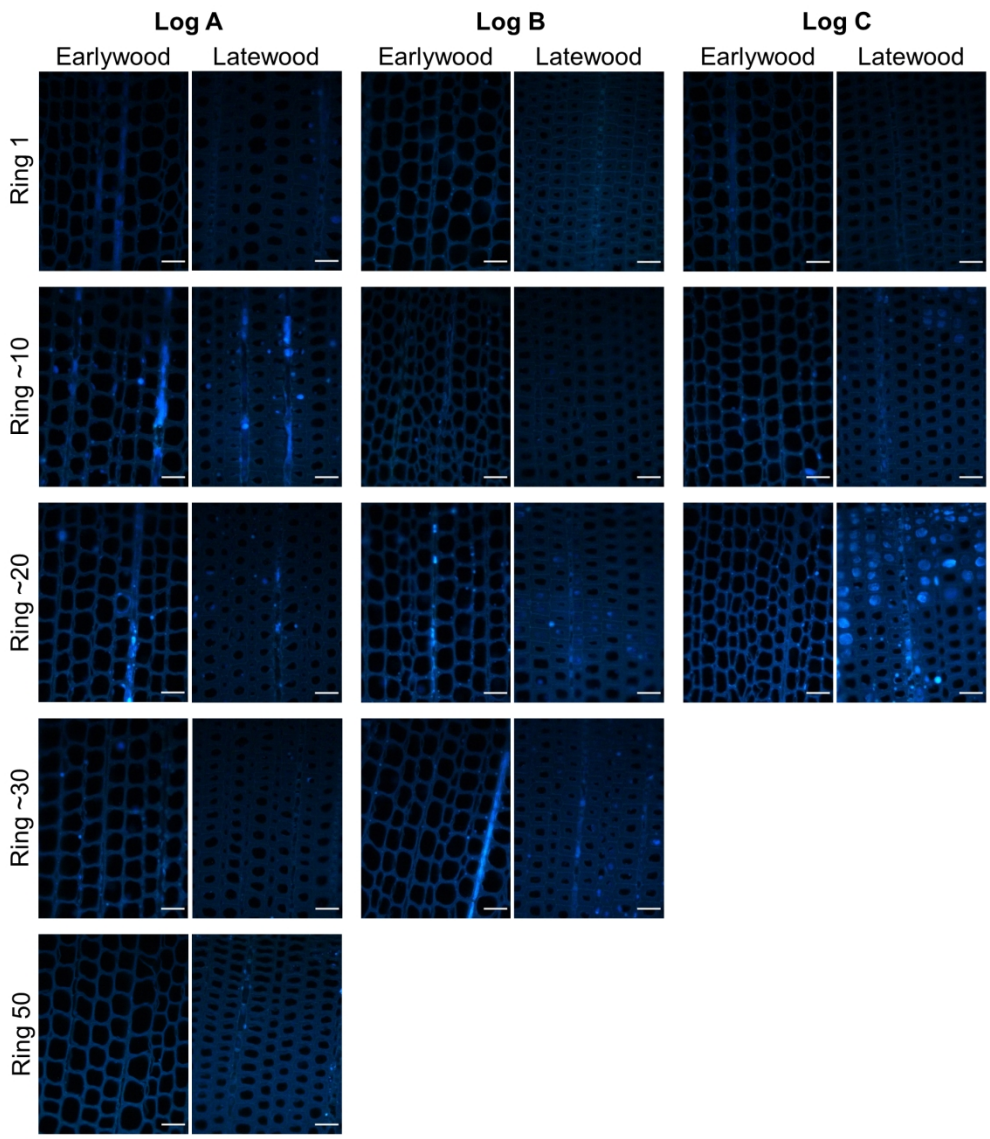

Figure 4. Fluorescence images (ex: 330-385 nm, em: 420- nm) showing the distribution of UV-fluorescent extractives in the earlywood and latewood regions of different heartwood annual rings in logs A, B and C. Ring 1 is the first ring at the sapwood-heartwood border designated as heartwood. Scale bar is 40 µm

171x197mm (300 x 300 DPI)

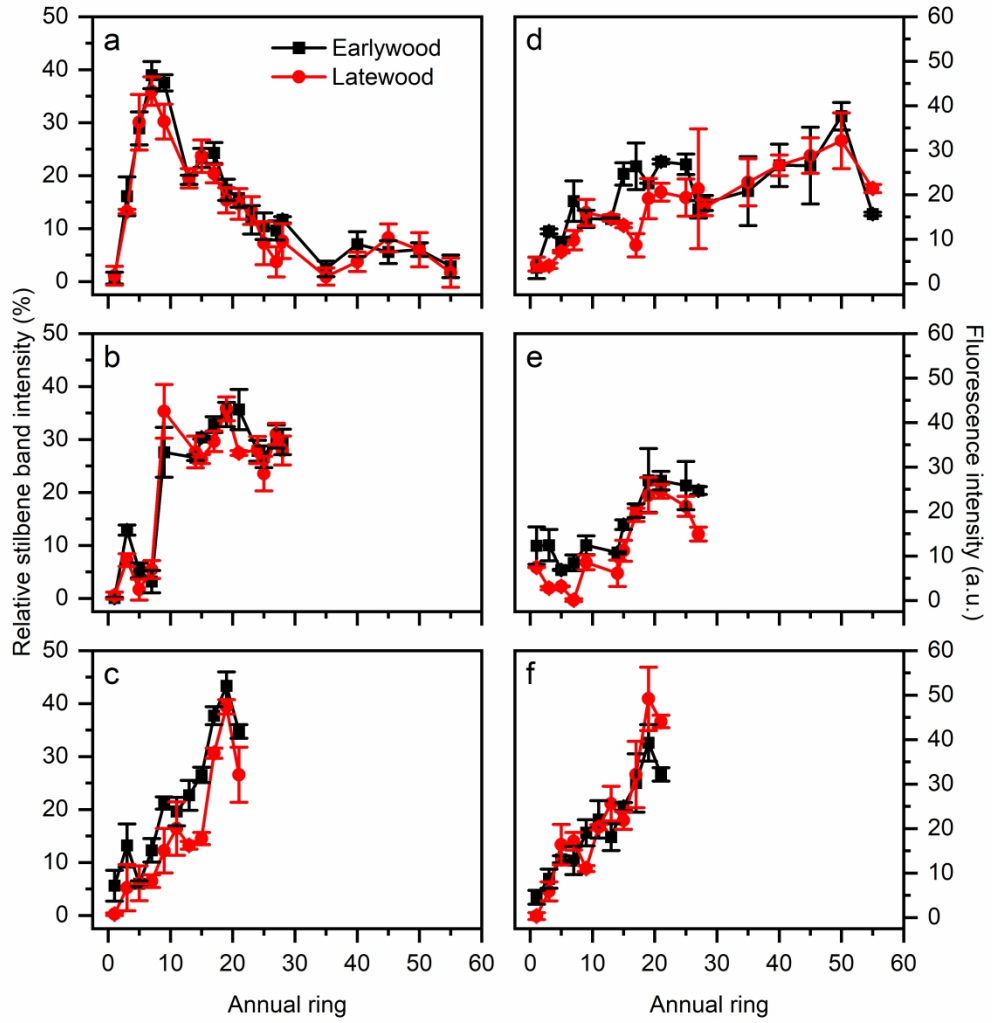

Figure 5. Relative stilbene band intensity (integrated intensity of the stilbene C=C stretch band at 1628-1645 rel. cm^{-1} relative to the integrated intensity of the aromatic ring stretch band at 1580-1620 rel. cm^{-1}) in the earlywood and latewood regions of different heartwood annual rings in logs A (a), B (b) and C (c), and fluorescence intensity (ex: 330-385 nm, em: 420- nm) in the earlywood and latewood regions of different heartwood annual rings in logs A (d), B (e) and C (f). Ring 1 is the first ring at the sapwood-heartwood border designated as heartwood. The relative stilbene band intensity is 0 in sapwood. The average fluorescence intensity of sapwood has been subtracted from the heartwood fluorescence values.

179x183mm (600 x 600 DPI)

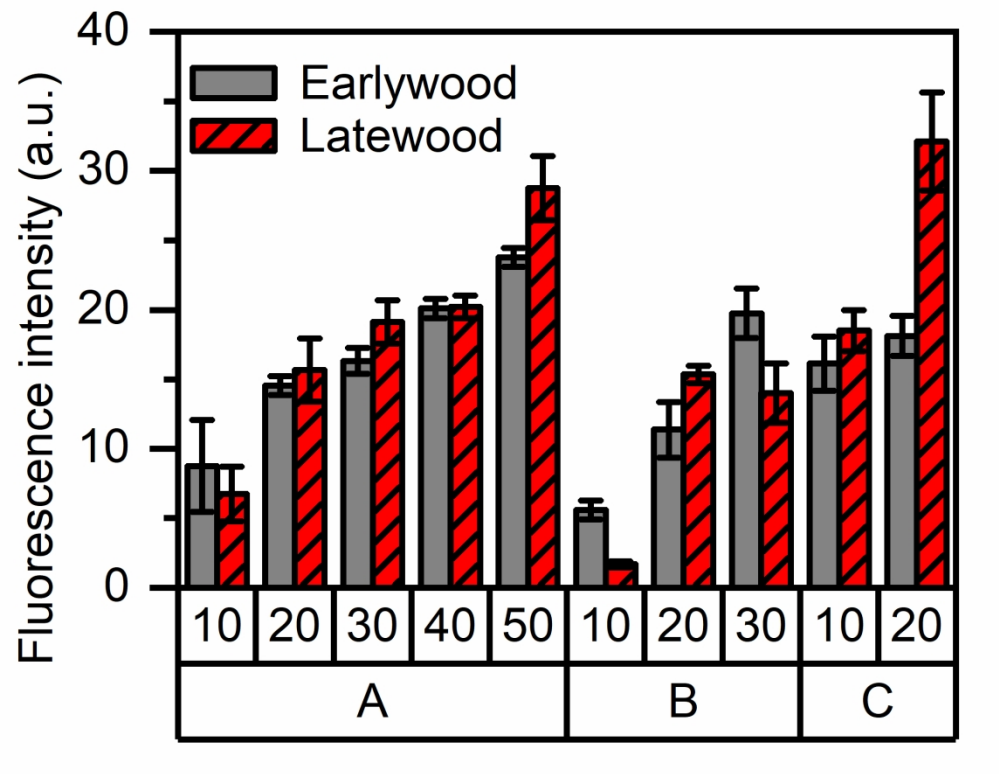

Figure 6. Fluorescence intensity (ex: 330-385 nm, em: 420- nm) after extraction in the earlywood and latewood regions of approximately every tenth heartwood annual ring in logs A, B and C. Ring 1 is the first ring at the sapwood-heartwood border designated as heartwood. The fluorescence intensity of sapwood has been subtracted from the heartwood fluorescence values

89x69mm (600 x 600 DPI)

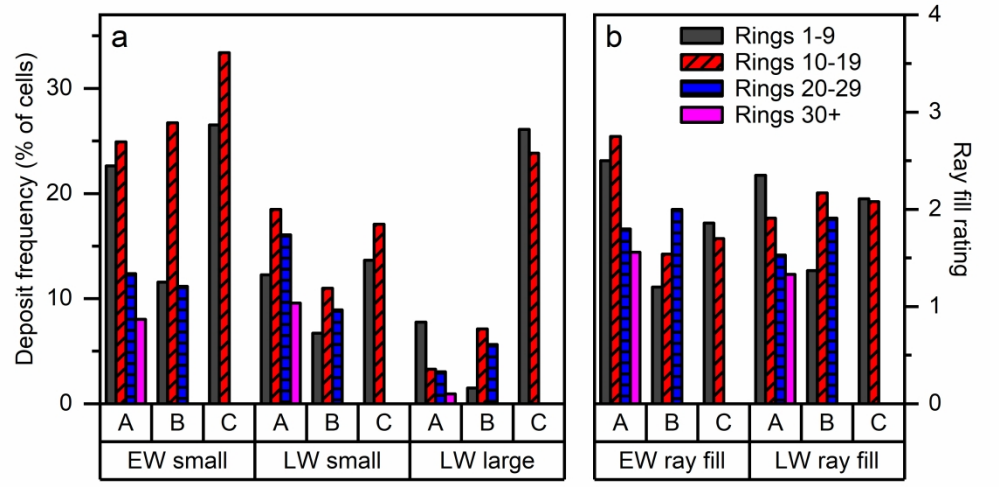

Figure 7. Frequency of small and large earlywood (EW) and latewood (LW) deposits in fluorescence images collected from different annual ring intervals in logs A, B and C (a), and the degree of ray filling in fluorescence images collected from different annual ring intervals in logs A, B and C given as ray fill rating, where 1 = 0-20% filling, 2 = 20-40% filling, 3 = 40-60% filling, 4 = 60-80% filling, and 5 = 80-100% filling (b)

179x87mm (600 x 600 DPI)

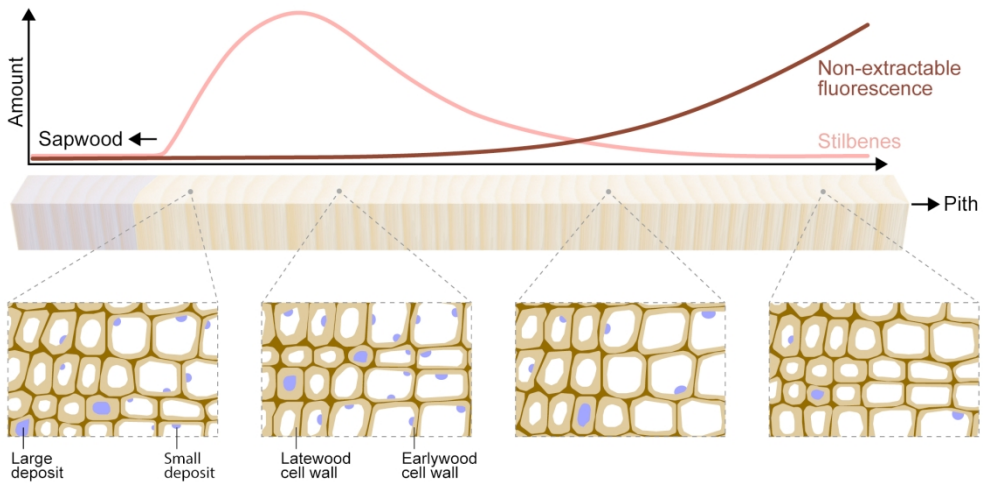

Figure 8. Stilbenes in Scots pine heartwood. Stilbene content increases for some 10-20 annual rings from the heartwood-sapwood border and then begins to decrease, along with a decrease in the abundance of stilbene-rich small deposits in tracheid lumens and an increase in non-extractable cell wall fluorescence. The large deposits found in latewood tracheid lumens contain mixtures of stilbenes and resin acids, and their abundance increases when the local resin acid content increases